The Effect of the Channel Head on the Unsteady Pressure Pulsation Characteristics at the Inlet and Outlet of Reactor Coolant Pumps

The Effect of the Channel Head on the Unsteady Pressure Pulsation Characteristics at the Inlet and Outlet of Reactor Coolant Pumps

Long Yun　Yin Junlian　Wang Dezhong[1]　**Hu Yaoyu**

School of Mechanical Engineering, Shanghai Jiao Tong University，
800 Dongchuan Road, Shanghai，200240，China

E-mail: longyunjs@sjtu.edu.cn

Abstract. In this paper, CFD approach was employed to analyse the inlet and outlet pressure pulsation characteristics of reactor coolant pumps with different inflows. The Reynolds-averaged Naiver-Stokes equations with the k-ε turbulence model were solved by the computational fluid dynamics software CFX to conduct the steady and unsteady numerical simulation. The numerical results of the straight pipe and channel head were validated with experimental data for the heads at different flow coefficients. In the nominal flow rate, the head of the pump with the channel head decreases by 1.19% when compared to the straight pipe. The channel head induces the inlet flow non-uniform, and the non-uniformity of the inflow induces the outlet flow of the pump with channel head different from that of the straight pipe. Meanwhile, the pressure pulsation signals are analysed using RMS, Standard Deviation and Peak-to-Peak Value method. At the points of the inlet and outlet, the pressure pulsation characteristics between the channel head and straight pipe are compared, and the difference is obviously. It is evident that the two different inflows of channel head and straight pipe have significant effect on the pump unsteady pressure pulsation. Finally, it is expected that the effects of non-uniform inflow on the pump performance and unsteady pressure pulsation are absolutely different from the uniform inflow. It is very important to provide accurate input conditions for the design and safety of the reactor.

1. Introduction
The reactor coolant pump is one of the most important equipment in nuclear power plant. In the APWR reactor primary coolant system, two canned motor pumps are directly attached to the cold side of the steam generator [1], as shown in Figure 1. The pumps are identical designs and are selected based on performance under uniform inflow with the straight pipe, but actually non-uniform suction flow is induced in the discharge pipe of the steam generator due to the complex geometry in the channel head, which might influence the performance of the pumps [2]. Unsteady flow problems in pumps may resonate with an acoustic mode of the inlet or discharging piping to produce a serious pulsation problem [3]. Furthermore, an effective approach should be developed to research pressure pulsation of the pumps with uniform and non-uniform inflow, which is sorely necessitated.

---

[1]　Wang Dezhong, professor，Email：dzwang@sjtu.edu.cn.

Up to now, only few researchers have studied the effect of the non-uniform inflow on the performance of the pumps. Van Esch B.P.M. et al. [4] investigated the performance of a mixed-flow pump and hydrodynamic forces on the impeller under non-uniform suction flow with experimental method, they found that the performance of the pump is influenced by the type of suction velocity profile and a considerable steady radial force appeared when the suction flow is non-uniform. Zhaofeng Xu et al. [5] studied the flow patterns of non-uniform flows, such as distribution of velocity, streamline, turbulence kinetic energy and vortex,in a rectangular open suction passage, by 2-D PIV method. Weidong Shi et al. [6] studied the effect of non-uniform suction flow on performance and pressure fluctuation in axial flow pump. Wei Huang et al, [7] investigated the flow characteristics within connection between steam generator channel head and pump suction by experimental method and found that the axial vortex is eliminated and axial velocity is uniform in the outlet section of the nozzle of the channel head. But the interaction between the channel head and the pump has not been investigated since no pumps are connected to the channel head in the test loop. And then, Cheng Hui, et al. [3] investigate the effect of the velocity distortion generated by the steam generator on the performance of the two pumps by CFD method, and the results suggest that the nozzle dam brackets should be installed in the outlet pipe of the steam generator.
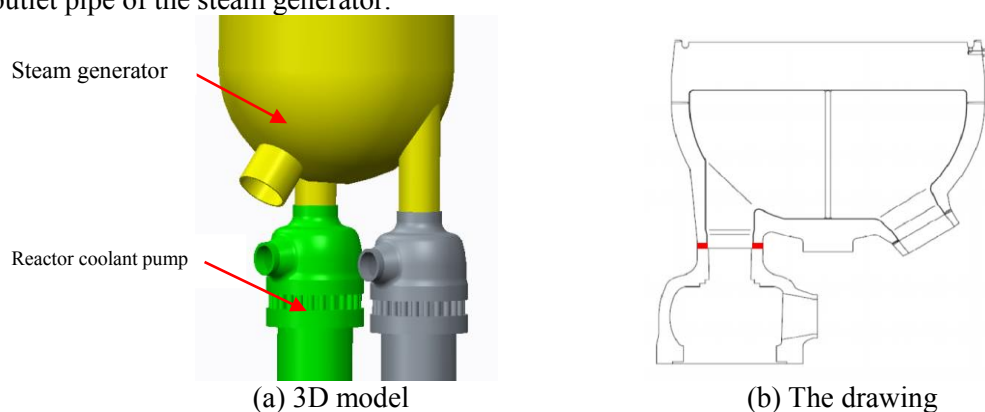

(a) 3D model   (b) The drawing
Figure 1. Schematic diagram of connection type

Generally, unsteady pressure pulsation induced by rotor–stator interaction, which excites mechanical vibrations of the pump, cannot be avoided entirely, even at the design operating condition. Up to now, lots of numerical and experimental investigations have been carried out, and the fast Fourier transform (FFT) method has been proved to be the most powerful tool to unveil the frequency characteristics of pressure fluctuations. Yao et al. [8] analysed both frequency domain and time-frequency domain in a double suction centrifugal pump based on fast Fourier transform (FFT) and time-frequency representation methods. Parrondo et al. [9] also investigated the unsteady pressure distribution in a conventional centrifugal pump, and particular attention was paid on pressure fluctuations at blade passage frequency. Some studies have laid their emphasis upon the influence of geometrical parameters on pressure pulsation characteristics by either experimental or numerical methods. Spence et al. [10] explored the effects of pressure pulsation. In their work, they took the form of a parametric study covering four geometric parameters by numerical analysis. And a rationalisation process aimed at reducing vibration through reductions in pressure pulsations has produced geometric recommendations. Yang et al. [11, 12] investigated unsteady pressure fields of the pump as turbine by numerical methods and illustrated that increasing blade tip clearance serves as an effective measure for reducing pressure pulsation. Benra et al. [13] investigated the periodic unsteady flow in a single-blade pump by CFD simulation and particle image velocimetry measurement method, and the results showed that transient numerical simulations compare very well to velocity measurements. Pei et al [14, 15] conducted the numerical investigation on the periodically unsteady flow of a single-blade pump and predicted the flow in a whole passage. Toussaint et al. [16] conducted experimental investigation on the unsteady flow in a centrifugal pump in off-design operating conditions and concluded that the pressure fluctuations took place at blade passing frequency, rotation frequency, and their harmonics.

Zhang et al. [17] explored an effective method to reduce high pressure pulsation level by investigating a slope volute pump, and analysed its influence on flow structures using numerical simulation.

Therefore, the major aim of this study is to employed CFD approach to simulate the unsteady flow field of a scaled model reactor coolant pump with uniform and non-uniform inflow conditions, then to investigate the inlet and outlet unsteady pressure pulsation. The three-dimensional pump internal flow channel was modelled by pro/E software, Reynolds-averaged Naiver-Stokes equations with the k-ε turbulence model were solved by the computational fluid dynamics software CFX to conduct the steady and unsteady numerical simulation, by which the flow field and pressure pulsations were obtained. The special attention is paid to compare pressure pulsation characteristics value with different inflows.

2. Numerical Simulation

2.1. The pump model
The two model pumps are identical designs, and the parameters of the pump are shown in Table 1. Nominal flow rate and head of the model pump is 950 m^3/h and 13.5 m, respectively. Figure 1 shows the cold side of the steam generator with two discharge pipes. Since the cold side of the steam generator is symmetrical, it is assumed that the flow field inside is also symmetrical. So the channel head could be divided into two mirror parts. The effect of the channel head and straight pipe on the performance of the pump can be investigated individually. The computational domain includes the channel head, straight pipe, impeller, diffuser, spherical casing with straight outlet pipe, as shown in Figure 2.
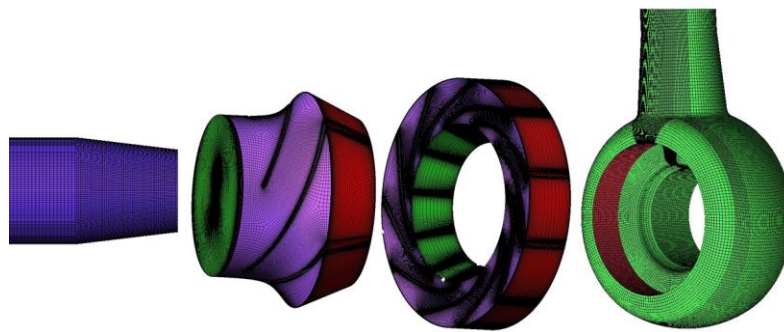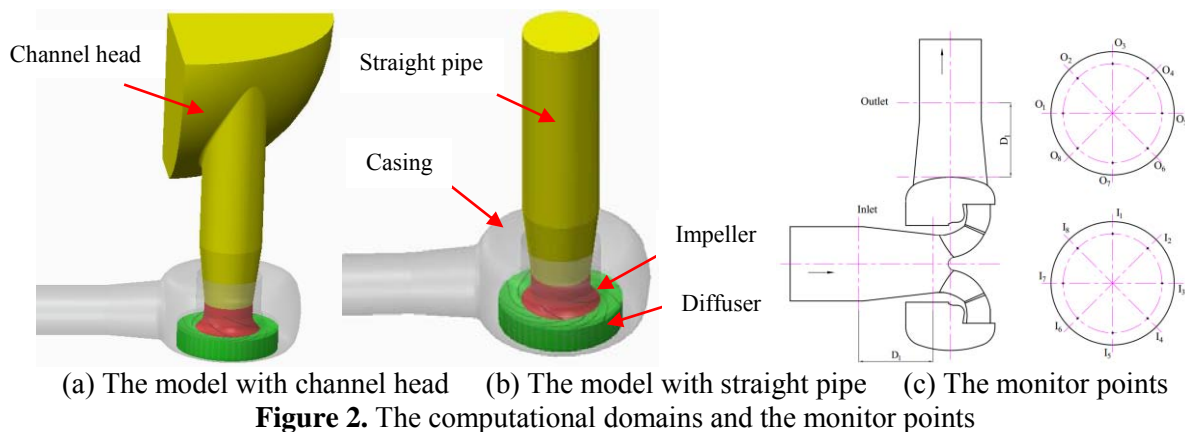
Table 1. Nomenclature

Parameter	Value	Parameter	Value
Impeller outlet diameter D_2	271.5 mm	Tangential velocity of impeller outlet u_2	21.03 m/s
Impeller outlet width b_2	83 mm	Impeller blade number Z_1	5
Rotating speed n_d	1480 r/min	Diffuser blade number Z_2	11
Angular velocity ω	155 rad/s	Nominal flow rate coefficient Φ_d	$Q_d/(\omega D_2^2 b_2)$
Inlet pipe diameter D_1	300 mm	Nominal head coefficient Ψ_d	$gH_d/(\omega^2 d_2^2)$
Pressure amplitude p	Pa	Specific speed	387.5
Pressure coefficient C_p	$p/0.5\rho u_2^2$	Water density ρ	1000 kg/m^3

2.2. The monitor point
In order to monitor the unsteady pressure pulsation in the inlet and outlet of the model pump, the points of I_1~I_8 are set at the inlet section apart from the impeller a distance of D_1, and the points of O_1~O_8 are set at the outlet section apart from the impeller a distance of D_1, as shown in Figure 2(c).

2.3. The mesh
In order to improve the grids quality, nearly all the computational domains are meshed by the hexahedral elements, except for the channel head with complex geometry. The grids of the impeller, diffuser and casing are shown in Figure 3. The magnitude of y+ around the blades is lower than 200. The straight pipe grid number is 1,214,400, the channel head grid number is 1,967,476, impeller grid number is 1,132,405, the diffuser grid number is 1,919,775, and the casing grid number is 1,276,405.

(a) The model with channel head   (b) The model with straight pipe   (c) The monitor points
Figure 2. The computational domains and the monitor points

Figure 3. The grids of each component

2.4. The boundary condition
To obtain a stable numerical simulation, an initial value distribution of the flow parameters used as exactly as possible was required. The working medium is water at 25℃. The rotation of the impeller is set to be 1480r/min. The mass flow rate at inlet and the pressure at outlet are set as the boundary condition. The *k-ε* turbulent model is chosen to solve RANS equation. The adiabatic and no-slip boundary condition is applied to the solid walls. The residual convergence precision of the steady calculation is set to 10^{-4}. The second-order backward Euler scheme is chosen for the time discretization. The interface between the impeller and the casing is set to "transient rotor-stator" to capture the transient rotor-stator interaction in the flow. The chosen time step Δt for the transient simulation is 3.3784×10^{-4} s for the nominal rotating speed, corresponding to the changed angle of 3° of impeller rotation. Therefore, 120 transient results are included for one impeller revolution calculation. Ten revolutions of the impeller for the design condition are conducted. Within each time step, the number of iterations has been chosen to 25 and the iteration stops when the maximum residual is less than 10^{-4}.

3. Results and Discussions

3.1. Hydraulic performance
Figure 4 shows the pump hydraulic performance of different suction flows and experiment, and the experiment is conducted with the straight pipe. The numerical results of the straight pipe and channel head were validated with experimental data for the heads at different flow coefficients. The heads of the pump at $0.8\Phi_d$, $1.0\Phi_d$, $1.2\Phi_d$ compared with CFD and experiment were shown in Table 2. H_C means the head of the pump with the channel head, H_S means the head of the pump with the straight pump, H_{exp} means the head of the pump by experiment. It can be concluded that the suction flow coming from the channel head of the steam generator has a considerable effect on the performance of the canned motor pumps.
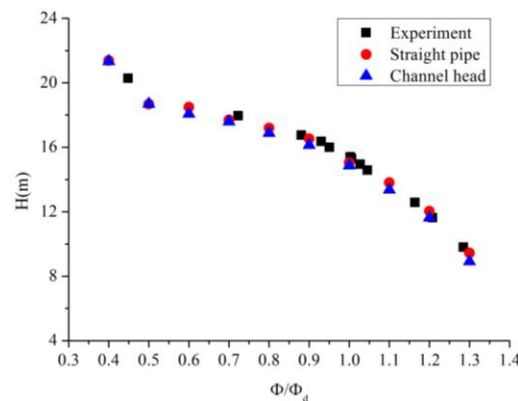
Figure 4. The head curve of the pump compared with CFD and experiment

Table 2. The head of the pump compared between with CFD and experiment

Φ/Φ_d	H_{exp}(m)	H_C(m)	H_S(m)	$(H_C-H_{exp})/H_{exp}$(%)	$(H_S-H_{exp})/H_{exp}$(%)	$(H_C-H_S)/H_S$(%)
0.8	17.365	16.878	17.195	-2.804	-0.978	-1.844
1.0	15.400	14.859	15.039	-3.511	-2.347	-1.192
1.2	11.801	11.629	12.031	-1.460	1.952	-3.347

3.2. Flow field analysis

To clarify the reason leading to the difference of pump performance with different inflow, Figure 5 presents the velocity distributions in the channel head and straight pipe. In Figure 5(a), at nominal flow rate, the velocity distribution in the channel head is non-uniform, and the velocity distribution in the straight pipe is uniform. In Figure 6(a) and (b), the low pressure region at the outlet with the straight pipe is obviously different from the channel head, and the pressure field structure at the outlet with the straight pipe is overall different from the channel head. Compared with Figure 7(a) and Figure 7(b), the low velocity region with the straight pipe mainly is at the top, and the low velocity region with the channel head mainly is at the right. It is evident that the two different inflows of channel head and straight pipe induce the difference of inlet flow, the channel head induces the inlet flow non-uniform, and the non-uniformity of the inflow induces the outlet flow with channel head different from that with the straight pipe. The reason for the variation of pump performance is probably related to inflows structures of the pump with the channel head and straight pipe.
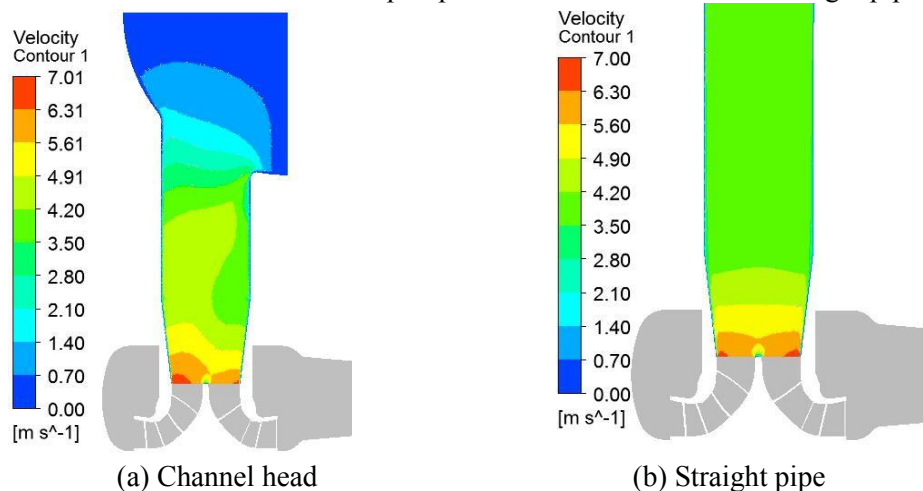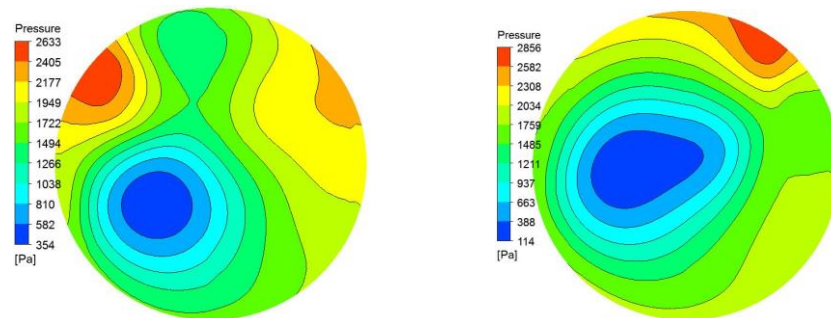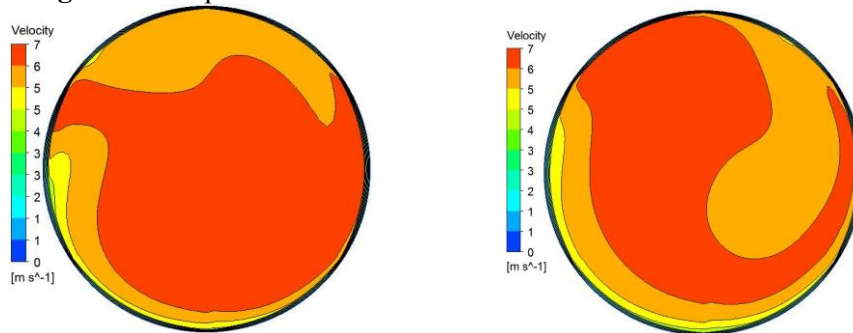

(a) Channel head   (b) Straight pipe

Figure 5. The velocity distributions in the channel head and straight pipe

(a) Channel head   (b) Straight pipe

Figure 6. The pressure distribution at the outlet with different inflow

(a) Channel head   (b) Straight pipe

Figure 7. The velocity distribution at the outlet with different inflow

3.3. Unsteady pressure pulsation at the inlet and outlet of the model pump

Unsteady pressure pulsation simulations of the model pump were conducted at the inlet and outlet in the design flow rates. To evaluate pressure pulsation energy in particular frequency band, Standard Deviation (SD) method, Root Mean Square (RMS) and Peak-to-Peak Value (VPP) method were applied to deal with discrete pressure signals as presented in Eq. (1)~(6),

$$SD = \sqrt{\frac{1}{n}\sum_{i=1}^{n}(\frac{1}{0.5\rho u_2^2}A_i - \overline{A})^2} \tag{1}$$

$$\overline{A} = \frac{1}{0.5\rho u_2^2}\frac{1}{n}\sum_{i=1}^{n}A_i \tag{2}$$

$$RMS = \frac{1}{0.5\rho u_2^2}\sqrt{\frac{1}{n}\sum_{i=1}^{n}A_i^2} \tag{3}$$

where A_i represents pressure amplitudes at different frequencies, and $\overline{A}$ is mean amplitude.

$$VPP = Y_{max} - Y_{min} \tag{4}$$

$$Y_{max} = \frac{1}{0.5\rho u_2^2}MAX(A_1, A_2, ..., A_n) \tag{5}$$

$$Y_{min} = \frac{1}{0.5\rho u_2^2}MIN(A_1, A_2, ..., A_n) \tag{6}$$

where Y_{max} represents the maximum value of all data, Y_{min} represents the minimum value of all data. The characteristic value of pressure pulsation at the inlet monitor points with the channel head and straight pipe are shown in Figure 8. As illustrated in Figture 8(a), the *SD* at I_1~I_8 with the channel

head changes very little, the *SD* at $I_1 \sim I_8$ with the straight pipe also changes very little, and the *SD* of the channel head is almost 10.4% lower than the straight pipe. In Figure 8(b), the Y_{min} with the channel head has the lagerest value at I_4 point and the least value at I_7 point, the Y_{min} at $I_1 \sim I_8$ with the straight pipe changes very little, and it is the largest difference that the Y_{min} of the channel head is 0.674% higher than the straight pipe and the least difference that the Y_{min} of the channel head is 0.009% lower than the straight pipe. Similar to the Y_{min}, the Y_{max} with the channel head has the lagerest value at I_4 point and the least value at I_7 point, the Y_{max} at $I_1 \sim I_8$ with the straight pipe changes very little, and it is the largest difference that the Y_{max} of the channel head is 0.848% higher than the straight pipe and the least difference that the Y_{max} of the channel head is 0.138% higher than the straight pipe, as shown in Figture 8(c). Figture 8(d) shows the mean value $\bar{A}$ at $I_1 \sim I_8$ with the straight pipe and channel head, the $\bar{A}$ with the channel head has the lagerest value at I_4 point and the least value in I_7 point, the $\bar{A}$ at $I_1 \sim I_8$ with the straight pipe changes very little, and it is the largest difference that the $\bar{A}$ of the channel head is 0.731% higher than the straight pipe and the least difference that the $\bar{A}$ of the channel head is 0.035% higher than the straight pipe. As illustrated in Figture 8(e), the *VPP* at $I_1 \sim I_8$ with the channel head changes very little, the *VPP* at $I_1 \sim I_8$ with the straight pipe also changes very little, and the *VPP* of the channel head is almost 4.42% lower than the straight pipe. In Figture 8(f), the *RMS* with the channel head has the lagerest value at I_7 point and the least value in I_4 point, the *RMS* at $I_1 \sim I_8$ with the straight pipe changes very little, and it is the largest difference that the *RMS* of the channel head is 0.730% higher than the straight pipe and the least difference that the *RMS* of the channel head is 0.034% higher than the straight pipe.

(a) *SD*   (b) Y_{min}

(c) Y_{max} (d) $\bar{A}$
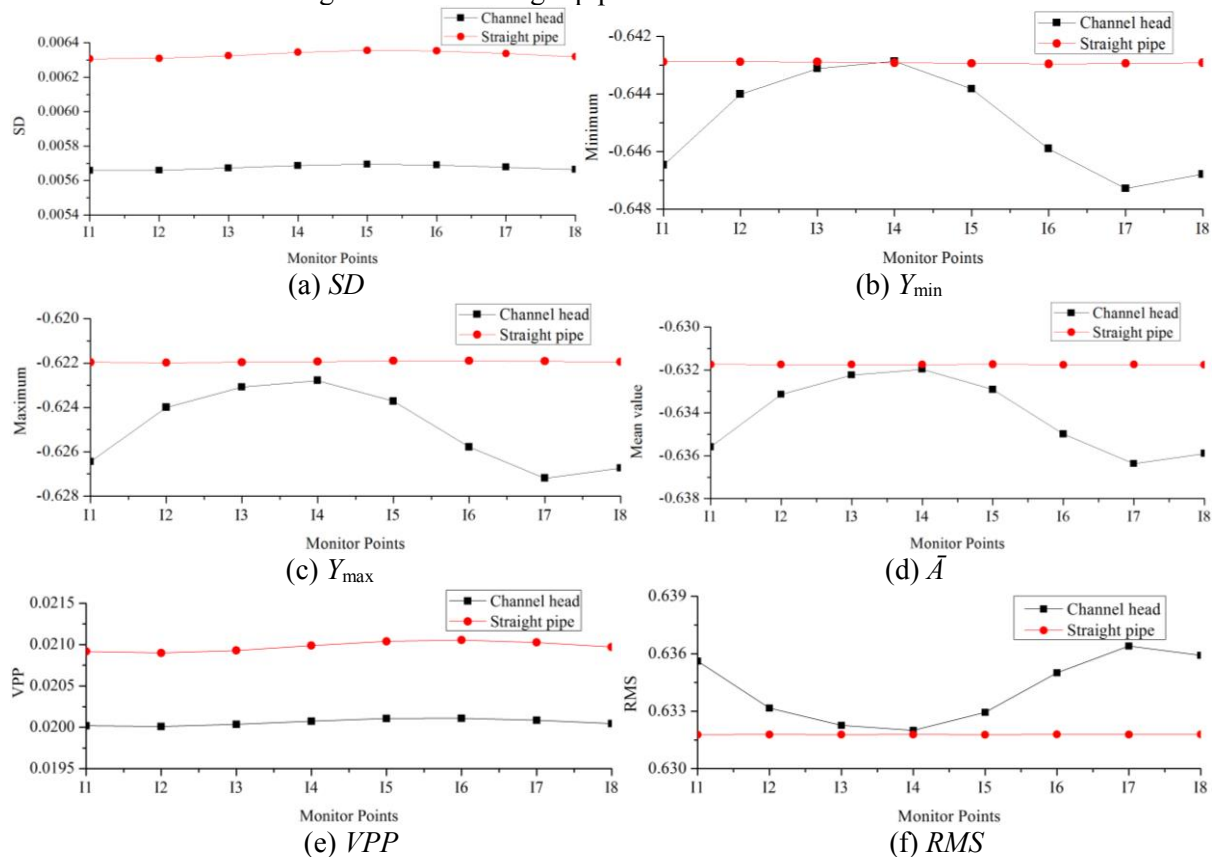
(e) *VPP*   (f) *RMS*

Figure 8. The characteristic value of pressure pulsation with different suction flows at inlet

The characteristic value of pressure pulsation at the outlet monitor points with the channel head and straight pipe are shown in Figure 9. As illustrated in Figture 9(a), the *SD* at $O_1 \sim O_8$ with the channel head changes very little, the *SD* at $O_1 \sim O_8$ with the straight pipe changes a lot and has the lagerest value at O_4 point, it is the largest difference at O_4 point that the *SD* of the channel head is 14.289% lower than the straight pipe, and it is the least difference at O_7 points that the *SD* of the channel head is

0.307% lower than the straight pipe. In Figure 18(b), the Y_{min} with the channel head has the lagerest value at O_4 point and the least value at O_1 point, the Y_{min} with the straight pipe has the lagerest value at O_6 point and the least value at O_1 point, and it is the largest difference at O_1 point that the Y_{min} of the channel head is 39.587% higher than the straight pipe and the least difference at O_5 point that the Y_{min} of the channel head is 1.867% lower than straight pipe. Similar to the Y_{min}, the Y_{max} with the channel head has the lagerest value at O_4 point and the least value at O_1 point, the Y_{max} with the straight pipe has the lagerest value at O_4 point and the least value at O_1 point, and it is the largest difference at O_3 point that the Y_{max} of the channel head is 18.346% lower than the straight pipe and the least difference at O_5 point that the Y_{max} of the channel head is 2.552% lower than the straight pipe, as shown in Figure 9(c). Figure 9(d) shows the mean value $\bar{A}$ at $O_1 \sim O_8$ with the straight pipe and channel head, the $\bar{A}$ with the channel head has the lagerest value at O_4 point and the least value in O_1 point, the $\bar{A}$ with the straight pipe has the lagerest value at O_6 point and the least value at O_1 point, and it is the largest difference at O_1 point that the $\bar{A}$ of the channel head is 21.630% higher than the straight pipe and the least difference that the $\bar{A}$ of the channel head is 3.211% lower than the straight pipe. As illustrated in Figure 9(e), the *VPP* with the channel head has the lagerest value at O_7 point and the least value at O_1 point, the *VPP* with the channel head changes a little, the *VPP* with the straight pipe has the lagerest value at O_4 point and the least value at O_6 point, and it is the largest difference at O_4 point that the *VPP* of the channel head is 14.289% lower than the straight pipe and the least difference at O_5 point that the *VPP* of the channel head is 0.307% lower than the straight pipe. In Figure 9(f), the *RMS* with the channel head has the lagerest value at O_4 points and the least value in O_1 points, the *RMS* with the straight pipe has the lagerest value at O_6 point and the least value at O_1 point, and it is the largest difference at O_1 point that the *RMS* of the channel head is 20.751% higher than the straight pipe and the least difference that the *RMS* of the channel head is 3.197% lower than the straight pipe. At the points of the inlet and outlet, the difference of the pressure pulsation characteristic value between the channel head and straight pipe are obviously.
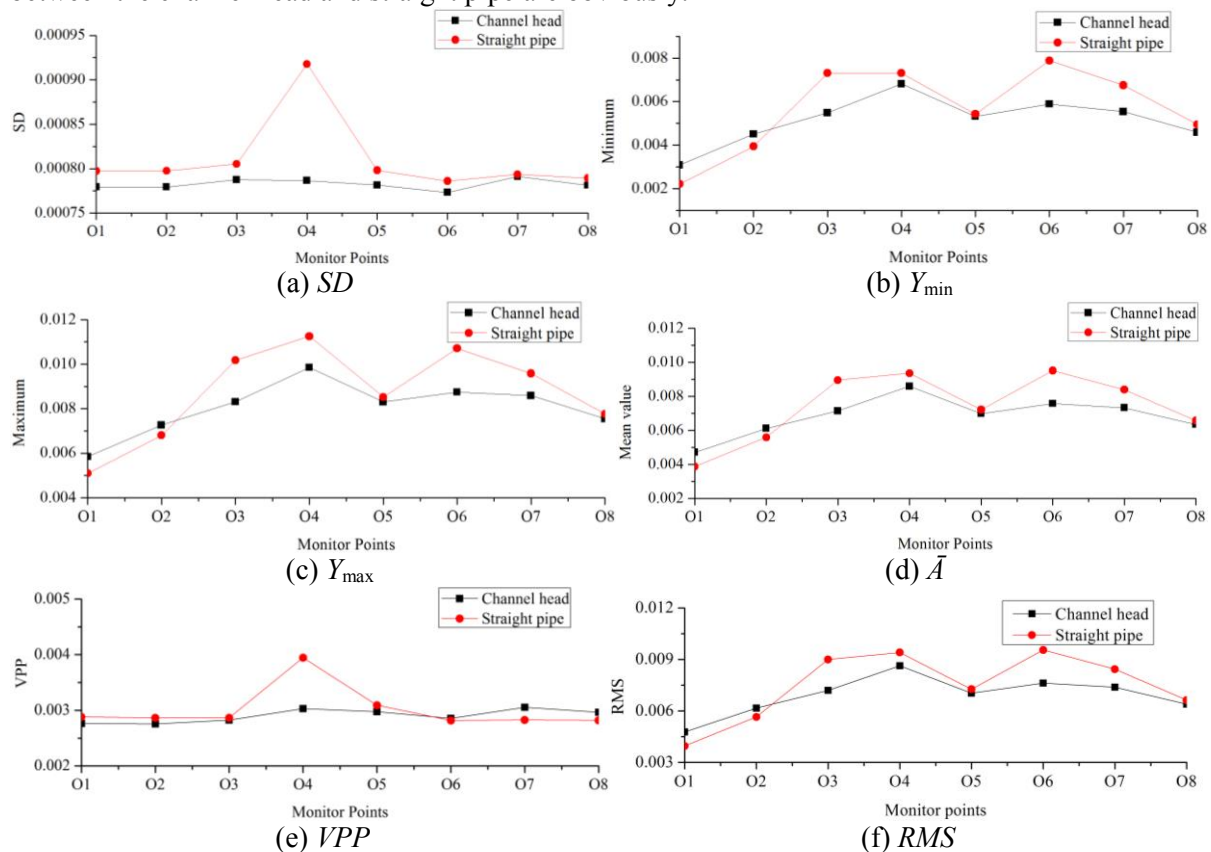

(a) *SD*   (b) Y_{min}

(c) Y_{max} (d) $\bar{A}$

(e) *VPP*   (f) *RMS*

Figure 9. The characteristic value of pressure pulsation with different suction flows at outlet

4. Conclusion

In this paper, the numerical analysis on unsteady pressure pulsation features of a scaled model reactor coolant pump with different inflows is presented. The pump head with the straight pipe measured by experimental method is compared to that of the channel head and the straight pipe obtained by numerical method. The analysis focuses on the flow fields and pressure pulsations at positions of the inlet and outlet in the nominal flow rate. Pressure pulsation signals are analysed using RMS, Standard Deviation and Peak-to-Peak Value method.

The numerical results of the straight pipe and channel head were validated with experimental data for the heads at different flow coefficients. In the nominal flow rate, the head of the pump with the channel head decreases by 1.19% when compared to the straight pipe. The channel head induces the inlet flow non-uniform, and the non-uniformity of the inflow induces the outlet flow of the pump with channel head different from that of the straight pipe.

Meanwhile, the pressure pulsations of different inflows are investigated. The global instability inflow induces rather high amplitude pressure pulsation. At the points of the inlet and outlet, the pressure pulsation characteristics between the channel head and straight pipe are compared, and the difference is obviously. It is evident that the two different inflows of channel head and straight pipe have significant effect on the pump unsteady pressure pulsation.

Finally, it is expected that the effects of non-uniform inflow on the pump performance and unsteady pressure pulsation are absolutely different from the uniform inflow. It is very important to provide accurate input conditions for the design and safety of the reactor.

Reference

[1] SUN, H.-h., CHENG, P.-d., and MIAO, H.-x., 2010, "The third generation of nuclear power technology AP1000," Beijing: China Electric Power Press.

[2] Cheng, H., Li, H., Yin, J., Gu, X., Hu, Y., and Wang, D., "Investigation of the distortion suction flow on the performance of the canned nuclear coolant pump."

[3] Brennen, C. E., "Hydrodynamics of pumps, 1994," Concepts ETI Inc., Oxford Science Publications, p. 81.

[4] Van Esch, B., 2009, "Performance and radial loading of a mixed-flow pump under non-uniform suction flow," Journal of Fluids Engineering, 131(5), p. 051101.

[5] Xu, Z., Yi, F., Liu, S., and Wu, Y., "2D PIV Experiments on Non-Uniform Flow in a Rectangular Open Model Pump Suction Passage," Proc. ASME 2005 International Mechanical Engineering Congress and Exposition, American Society of Mechanical Engineers, pp. 523-530.

[6] Huang, W., Zhang, W.-q., Tao, W.-q., He, J.-s., Huang, H., Zhang, F.-y., and Liu, X.-b., 2002, "Flow Characteristics Experimental Study within Connectionbetween Steam Generator Channel Head and Pump Suction," Nuclear Power Engineering, 23(2; SUPP), pp. 38-42.

[7] Yao, Z., Wang, F., Qu, L., Xiao, R., He, C., and Wang, M., 2011, "Experimental investigation of time-frequency characteristics of pressure fluctuations in a double-suction centrifugal pump," Journal of Fluids Engineering, 133(10), p. 101303.

[8] Parrondo-Gayo, J. L., Gonzalez-Perez, J., and Fernández-Francos, J. n., 2002, "The effect of the operating point on the pressure fluctuations at the blade passage frequency in the volute of a centrifugal pump," Journal of Fluids Engineering, 124(3), pp. 784-790.

[9] Spence, R., and Amaral-Teixeira, J., 2009, "A CFD parametric study of geometrical variations on the pressure pulsations and performance characteristics of a centrifugal pump," Computers & Fluids, 38(6), pp. 1243-1257.

[10] Yang, S.-S., Kong, F.-Y., Chen, H., and Su, X.-H., 2012, "Effects of blade wrap angle influencing a pump as turbine," Journal of Fluids Engineering, 134(6), p. 061102.

[11] Yang, S.-S., Liu, H.-L., Kong, F.-Y., Xia, B., and Tan, L.-W., 2014, "Effects of the radial gap between impeller tips and volute tongue influencing the performance and pressure pulsations of pump as turbine," Journal of Fluids Engineering, 136(5), p. 054501.

[12] Benra, F.-K., 2006, "Numerical and experimental investigation on the flow induced oscillations of a single-blade pump impeller," Journal of Fluids Engineering, 128(4), pp. 783-793.

[13] Pei, J., Yuan, S., Benra, F.-K., and Dohmen, H. J., 2012, "Numerical prediction of unsteady pressure field within the whole flow passage of a radial single-blade pump," Journal of Fluids Engineering, 134(10), p. 101103.

[14] Pei, J., Yuan, S., and Yuan, J., 2013, "Numerical analysis of periodic flow unsteadiness in a single-blade centrifugal pump," Science China Technological Sciences, 56(1), pp. 212-221.

[15] Toussaint, M., "Analysis of unsteady flow in centrifugal pump at off-design point operation," Proc. Proceeding of 23rd IAHR Symposium on Hydraulic Machinery and Systems, Yokohama, Japan, Paper.

[16] Zhang, N., Yang, M., Gao, B., Li, Z., and Ni, D., 2015, "Experimental investigation on unsteady pressure pulsation in a centrifugal pump with special slope volute," Journal of Fluids Engineering, 137(6), p. 061103.